International Research Journal on Advanced Engineering and Management
https://goldncloudpublications.com
https://doi.org/10.47392/IRJAEM.2025.0387
e ISSN: 2584-2854
Volume: 03
Issue:07 July 2025
Page No: 2456 - 2469

Heat Radiation Affects Hydro Magnetic Flow in A Spinning Porous Disc Within a Heat-Producing and Absorbing Medium

R. Umadevi[1], M. Gomathi[2], D. Arivukkodi[3], K. Vijayalakshmi[4], R. Sumathy[5]
[1,4]Assistant Professor, Department of Mathematics, Sri Venkateswara College of Engineering, Sriperumbudur, India.
[2,5]Research Scholar, Department of Mathematics, Sri Venkateswara College of Engineering, Sriperumbudur, India.
[3]Assistant Professor, Department of Mathematics, St. Joseph's College of Engineering, OMR, Chennai, India.
Email ID: *rumadevi13@gmail.com[1], gomathimaths11@gmail.com[2], arivukkodi.karthikeyan@gmail.com[3], viji15arvind@gmail.com[4], sumathyvedh2223@gmail.com[5]*

Abstract
This study examines the impact of thermal radiation on the electrically conducting grey fluid's continuous laminar convective hydromagnetic flow over a rotating porous disk in a porous medium, using an external uniform magnetic field and heat generation/absorption. When the disc is placed in a perpendicular magnetic field, a uniform suction should be expected over its surface. A solution to a nonlinear ordinary differential equation can be obtained by applying the suitable similarity transformation suggested by von Karman to the controlling nonlinear partial differential equations. Everything related to heat transfer is covered here, including situations with prescribed surface temperature (PST) and prescribed heat flux (PHF). The numerical solutions are visually shown by graphs. These solutions are obtained by a fourth-order Runge-Kutta based shooting method. Fluid temperature and velocity, as well as the Prandtl number, heat produced or absorbed, medium porosity, suction parameter, and radiation parameter are all investigated in detail in this area. These impacts are illustrated via graphs. Results for different parameters are included in tables along with the corresponding Nusselt number and skin-friction coefficients. Consistent with the sources mentioned before, all of the results are in agreement.

Keywords: *Radiation, Thermal Conduction, Rotating Disk, Laminar Flow, PST, PHF*

1. Introduction
Numerous applications have laminar spinning discs under investigation, such as rotors, turbines, jet engines, flywheels, vehicles, pumps, compressors, and a host of others. As described by Takhar et al. [1], when an axisymmetric body spins in a forced flow field caused by centrifugal force, fluid is propelled radially from almost all surfaces of the body. Following that, the axially flowing fluid assumes its place. Consequently, at a spinning body the fluid's axial velocity is greater than at a stationary one. Improving the fluid's convective heat transport from the body is achieved by increasing its axial velocity. To improve heat transport, practical solutions have been developed based on this principle. To illustrate the practicality of spinning condensers for spacecraft power plants and seawater distillation in a zero-gravity environment, Hickman [2] conducted experiments. Scholars have primarily focused on the initial rotating disc problem, which was introduced by von Karman [3]. Everything revolves around a disc that spins endlessly, even if the fluid is at rest far away from the disc. The flow is viscous. This extends the problem to include cases when the fluid is a solid body spinning above the disc, with injection or suction at the disc surface. There have been several theoretical, numerical, and empirical attempts to solve the stability and spinning disc problems, with names like [4] – [7] among them.

International Research Journal on Advanced Engineering and Management
https://goldncloudpublications.com
https://doi.org/10.47392/IRJAEM.2025.0387
e ISSN: 2584-2854
Volume: 03
Issue:07 July 2025
Page No: 2456 - 2469

The following is a synopsis of the publicly available literature on the subject to aid readers in understanding the scope and context of the work. Discs with holes in them that spin constantly produce laminar convective flows with unique characteristics, say Maleque and Sattar [8]. In his discussion of incompressible viscous fluid solutions in porous rotating disc flow, Turkyilmazoglu [9] reached a precise conclusion. Magneto hydrodynamic viscous flows have several technological uses, such as in high temperature plasmas, nuclear reactor cooling, magneto hydrodynamic (MHD) generators and accelerators, liquid metal fluids, and geothermal heat development. This has led to a surge of interest in studying how various geometries are affected by magnetic fields in terms of heat transfer and flow. Liquid metals, water with a little amount of acid, and other fluids displaying electrically conductive properties are all examples of what is meant here. While Kafoussias and Nanousis published their research on micropolar fluid MHD laminar boundary layer flow over a permeable wedge [11], Watanabe and Pop provided computational results of MHD free convection flow over a wedge in a magnetic field [10]. Expanding upon earlier research by Watanabe and Pop, Yih [12] accounts for the convection flow caused by MHD next to a non-isothermal wedge, taking into consideration magnetic and viscous dissipations, stress, and effort. Hydro magnetic flow induced by a rotating disc was examined by Attia and Hassan [13]. A lot of people in the research community have been interested in studying how heat moves through porous materials recently. But porous media are used in many industrial and geophysical processes. For small velocities, the Darcy model is typically employed. When the porosity level is high and the velocity is high, the Darcy-For chheimer drag force model must be used. Gaseous diffusion border cooling, filtration, energy systems, centrifuges, and magneto hydrodynamic convection from rotating discs and other substances imbedded in porous media have practical applications in these areas Hydromagnetic convection in porous media saturated with electrically conductive fluids has been the subject of a great number of regarded studies. Within a porous media, Rashad [14] investigated the effects of thermosphoretics and thermal radiation on hydromagnetic free convection. Managing boundary layers and transpiration are two of the many practical uses of fluid flow over porous material borders. It is well-known that surface suction is one of the mechanisms that stabilizes fluid flows. A number of technical contexts, including ships, submarines, and spinning machinery, make use of suction in fluid dynamics to delay separation. This is crucial for controlling laminar turbulent flow on aircraft wings. Scientists Hassanien et al. [15] and [31] investigated the properties of mixed convection flow with respect to heat transmission using a flat plate embedded in a porous material. The same solutions for Hiemenz flow across porous surfaces are included in the explanation of mass movement and heat transfer via hydro magnetic mixed convection by Chamkha and Khaled [16]. Heat transmission and continuous flow through porous media over a rotating disc are two recent studies by Attia [17] and [33]. In addition, the ionization that occurs at high working temperatures might cause the fluid involved in radiative heat transfer to show electrical conductivity. Studying the impact of a magnetic field on this kind of flow is, hence, essential in areas of application where heat radiation and magneto hydrodynamics interact. In a nuclear reactor containment vessel, a magnetic field can be employed in a manner analogous to that of an electrical furnace to cool the first wall, therefore isolating the heated plasma from the wall. Due to methodological issues, our knowledge of how radiation influences the flow of a radiating fluid's boundary layer around a body is lacking. Researching fluid radiation has three primary obstacles. In radiative heat transfer, radiation is taken in by a system and subsequently released both internally and externally. This makes it very difficult to forecast how much fluid will be absorbed. Wavelength is the primary determinant of the absorption coefficients of fluids, both those that absorb and those that emit. An extremely difficult-to-process nonlinear partial differential equation is produced by adding radiation to the energy equation. A lot of research was done on how radiation affects convective fluxes. Researchers Hossain and Takhar [18] investigated the topic and examined the effects

International Research Journal on Advanced Engineering and Management
https://goldncloudpublications.com
https://doi.org/10.47392/IRJAEM.2025.0387
e ISSN: 2584-2854
Volume: 03
Issue:07 July 2025
Page No: 2456 - 2469

of radiation on the mixed convection flow of an optically dense, incompressible fluid over a heated vertical plate that maintains a constant surface temperature and free stream velocity. A study conducted by Hossain and Pop [19] examined the effects of radiation on the free convection of an optically dense, viscous, incompressible fluid as it flows down a heated, sloping, flat surface within a saturated porous medium that maintains a constant temperature. They assumed a suction boundary condition. The radiation effects on MHD flow were investigated by Abbas using a porous medium as an example [20]. Using the approximation of differential, Takhar et al. [21] examined gas dissipative radiative convection in a porous medium, a topic pertinent to geothermal energy systems. According to Chamkha [22], the goal of studying the dynamics of solar collectors was to determine how solar radiation affected the convection of medium that is permeable on an inclined plane. Mohammadein et al. [23] used the Rosseland model to study the impact of free convection in porous substrates with respect to radiative flux. There are some real-world situations where thermal radiation and internal heat generation/absorption can have a major impact on the rate of heat transmission from a heated surface [24] and [25]. Exothermic and endothermic chemical reactions can have an impact on fluids, for instance, due to their internal heat production and absorption [24] and [25]. Abo-Eldahab and Aziz [25] used the premise of internal heat generation and absorption to study hydromagnetic heat transport across a surface that is continuously expanding. In his research, Chamkha [26] examined the following: buoyancy, thermal radiation, heat generation or absorption, and continuous hydromagnetic boundary layer flow with an accelerating semi-infinite porous surface. In addition, researchers Molla et al. [27] and [32] investigated naturally occurring convection flows on a spherical surface that dissipate heat. Whether the boundary surface is subjected to a predetermined temperature or a predetermined heat flow determines the nature of the convective heat transfer. But many problems, particularly those involving the cooling of electrical and nuclear components, make use of the wall heat flux. Predicting the temperature of the wall, when the heat flow of the wall changes is one of the goals of heat transfer theory since overheating, burnout, and meltdown are significant challenges in these situations. Controlling the distribution of wall temperatures is the design's goal. Unlike surfaces with fixed wall temperatures, surfaces with a controlled heat flow rate are straightforward to measure in a lab and often used as approximations in practical settings. Inside this framework, the study of convection inside the boundary layer of a porous regime of a spinning disc is examined in connection with magnetic fields, creating or absorbing heat, as well as thermal radiation. More research is needed in this area, according to the authors, so the heat transfer community can get involved. Compared to the recent work in Reference [13], our attempt aims to improve upon it in two ways. Closed heat-transfer research addresses the cases where the heat flux (PHF) and surface temperature (PST) are required. Our focus is on how thermal radiation affects the distribution of temperatures. According to reference [28], there are a plethora of distinct similarity temperature treatments for PST and PHF cases. Initial estimates to address real-world physical difficulties are often based on these ideas. The research here presupposes that the sheet is hotter than the fluid. The goal of this effort is to tackle the nonlinear problem discussed earlier in a quantitative way.

2. Problem Statement in Mathematical Terms

Heat transmission is facilitated by a rotating porous disc, and this study examines radiation and internal thermal production /absorption in an incompressible, a steady stream of a uniform electrically conductive fluid moving around immersed in a porous substance is a cylindrical object. There is no change in the flow along the axis. In the positive z-direction, the fluid is presumed to extend indefinitely. For example, as depicted in Fig. I, let represent the polar coordinates of the cylinder. Additionally, while the disc is positioned at z = 0, let it rotate at a constant rotational velocity Ω. When increases, the velocity flow components become. Surface temperature of the revolving disk is kept steady. A distance calculating from the given surface, where the free stream is

International Research Journal on Advanced Engineering and Management
https://goldncloudpublications.com
https://doi.org/10.47392/IRJAEM.2025.0387
e ISSN: 2584-2854
Volume: 03
Issue:07 July 2025
Page No: 2456 - 2469

keeping up at a constant pressure P_∞ and temperature. The grey coloured fluid and has a Newtonian structure; it is also a heat sink and radiator. Assuming lesser 1 value of the magnetic Reynolds number, the uniform external field of magnetic is aligned perpendicular to the disk surface. Because the electrically conductive fluid's velocity generates a small induced magnetic field. Furthermore, a constant suction is maintained across the disk's surface across the whole range. (Figure 1)

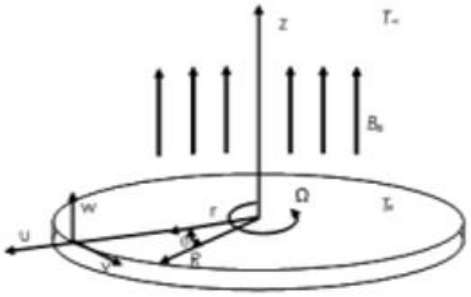

Figure 1 Schematic Diagram of the Problem

By making these assumptions, the following equations can be expressed to describe the energy, flow in a laminar incompressible boundary layer: momentum, continuity

$$\frac{\partial u}{\partial r}+\frac{u}{r}+\frac{\partial w}{\partial z}=0, \tag{1}$$

$$u\frac{\partial u}{\partial r}-\frac{v^2}{r}+w\frac{\partial u}{\partial z}+\frac{1}{\rho}\frac{\partial p}{\partial r}=\nu\left(\frac{\partial^2 u}{\partial r^2}+\frac{1}{r}\frac{\partial u}{\partial r}-\frac{u}{r^2}+\frac{\partial^2 u}{\partial z^2}\right)-\frac{\sigma B_0^2}{\rho}u-\frac{\mu}{K}u, \tag{2}$$

$$u\frac{\partial v}{\partial r}+\frac{uv}{r}+w\frac{\partial v}{\partial z}=\nu\left(\frac{\partial^2 v}{\partial r^2}+\frac{1}{r}\frac{\partial v}{\partial r}-\frac{v}{r^2}+\frac{\partial^2 v}{\partial z^2}\right)-\frac{\sigma B_0^2}{\rho}v-\frac{\mu}{K}v, \tag{3}$$

$$u\frac{\partial w}{\partial r}+w\frac{\partial w}{\partial z}+\frac{1}{\rho}\frac{\partial p}{\partial z}=\nu\left(\frac{\partial^2 w}{\partial r^2}+\frac{1}{r}\frac{\partial w}{\partial r}+\frac{\partial^2 w}{\partial z^2}\right)-\frac{\mu}{K}w, \tag{4}$$

$$u\frac{\partial T}{\partial r}+w\frac{\partial T}{\partial z}=\frac{\kappa}{\rho C_p}\left(\frac{\partial^2 T}{\partial r^2}+\frac{1}{r}\frac{\partial T}{\partial r}+\frac{\partial^2 T}{\partial z^2}\right)-\frac{1}{\rho C_p}\frac{\partial q_r}{\partial z}+\frac{Q}{\rho C_p}(T-T_\infty), \tag{5}$$

The constraints that define the problem's perimeter are given by

$$\left.\begin{aligned} &u=0,\ v=\Omega r,\ w=w_0, && \text{at } z=0,\\ &T=T_w=T_\infty+D_1\left(\frac{r}{l}\right)^2 && \text{(PST-case) at } z=0,\\ &-k\frac{\partial T}{\partial z}=q_w=D_2\left(\frac{r}{l}\right)^2 && \text{(PHF-case) at } z=0,\\ &u\to 0,\ v\to 0,\ T\to T_\infty,\ p\to p_\infty && \text{as } z\to\infty, \end{aligned}\right\} \tag{6}$$

released or absorbed as a function of volume, with the constant being, and radiative heat flux represented by q_r. An extremely opaque layer's radiation can be expressed using the Rosland approximation.

$$q_r=-\frac{4\sigma^*}{3\kappa^*}\frac{\partial T^4}{\partial z}, \tag{7}$$

since Stefan-Boltzmann's parameter and the coefficient of mean absorption are described by and respectively. This statement is stated as a linear function of temperature on the assumption that the flow's temperature changes are large enough. Accomplished this through broadening using Taylor series around neglecting terms with greater-order variables. Hence

$$T^4\cong 4T_\infty^3T-3T_\infty^4, \tag{8}$$

to (7) and (8), (5) becomes

3. Similarity Transformation

$$\left.\begin{aligned} &\eta=z(\Omega/\nu)^{\frac{1}{2}},\quad u=\Omega rF(\eta),\quad v=\Omega rG(\eta),\\ &w=(\Omega\nu)^{\frac{1}{2}}H(\eta),\quad p-p_\infty=2\mu\Omega P(\eta)\ \text{ and}\\ &T-T_\infty=\Delta T\theta(\eta)\qquad (PST-case)\\ &T-T_\infty=\frac{D_2}{k}\left(\frac{r}{l}\right)^2\sqrt{\frac{\nu}{\Omega}}\theta(\eta)\quad (PHF-case) \end{aligned}\right\} \tag{10}$$

Here a fluid's kinematic viscosity constant indicates by ν and, Eqs. (1) to (3) and (9) in the instance, by simplifying,

$$2F+H'=0, \tag{11}$$

$$F''-HF'-F^2+G^2-(\Lambda+M)F=0, \tag{12}$$

$$G''-HG'-2FG-(\Lambda+M)G=0, \tag{13}$$

$$\text{and}\quad \frac{\theta''}{Pr}\left(1+\frac{4}{3R_d}\right)-H\theta'+L\theta=0.\quad \text{(for PST \& PHF cases)} \tag{14}$$

Rephrasing the boundary conditions (6) as follows,

$$\left.\begin{aligned} &F(0)=0,\quad G(0)=1,\quad H(0)=W_s,\\ &\theta(0)=1\qquad \text{(PST-case)},\\ &\theta'(0)=-1\quad \text{(PHF-case)},\\ &F(\infty)=G(\infty)=\theta(\infty)=p(\infty)=0. \end{aligned}\right\} \tag{15}$$

While denotes for the magnetic parameter, represents the parameter for porosity, as the Prandtl number, indicates measure of radiation, is the heat generation coefficient or absorption and indicates a

International Research Journal on Advanced Engineering and Management
https://goldncloudpublications.com
https://doi.org/10.47392/IRJAEM.2025.0387
e ISSN: 2584-2854
Volume: 03
Issue:07 July 2025
Page No: 2456 - 2469

uniform suction parameter. The disk surface must adhere to the no-slip condition of viscous flow, as shown in equation (15). Equations (15) demonstrate that, apart from the induced axial component, all fluid velocities must vanish at a considerable distance from the disc surface. The three parts of the flow velocity can be found by solving the system of equations (11) through (14), using the boundary conditions given by equations (15). Equation (4) may be utilized to determine the pressure distribution if required. According to [30], when the fluid around a wall has a lower temperature than the wall itself, heat transfer takes place. The surface temperature is a necessary requirement for all energy problem boundary conditions of the disk be equal, as this is required by continuity concerns. becomes a great separation from the disc, here is the ambient fluid temperature. Following are the Newtonian formulas that can be used to calculate the Nusselt number and the coefficients of skin friction:

$$\tau_t = \left[\mu\left(\frac{\partial v}{\partial z} + \frac{1}{r}\frac{\partial w}{\partial \phi}\right)\right]_{z=0} = \mu G'\Omega(Re)^{\frac{1}{2}},$$

$$\tau_r = \left[\mu\left(\frac{\partial u}{\partial z} + \frac{1}{r}\frac{\partial w}{\partial \phi}\right)\right]_{z=0} = \mu F'\Omega(Re)^{\frac{1}{2}},$$

Therefore, regarding the two PST and PHF scenarios, radial and tangential skin frictions are provided by

$$(Re)^{\frac{1}{2}} C_{f_t} = G'(0), \quad (16)$$

$$(Re)^{\frac{1}{2}} C_{f_r} = F'(0), \quad (17)$$

For this particular PST case, the rate of heat transport is defined as

$$q = -\left(k\frac{\partial T}{\partial z}\right)_{z=0} = -k\Delta T\left(\frac{\Omega}{\nu}\right)^{\frac{1}{2}}\theta'(0), \quad (18)$$

Thus, Nusselt number is characterized as

$$(Re)^{-\frac{1}{2}} Nu = -\theta'(0). \quad (19)$$

Here represents Reynolds number of rotation.

4. Mathematical Methods for Resolving

Equations (11) to (14) are second-order, highly non-linear boundary value issues. Thus, the ideal numerical shooting method is formulated by utilizing the 4th order Runge-Kutta integration technique. The procedure commences with an initial estimate value η and proceeds by employing a specific set of parameters to resolve the problem and derive F ′(0), G ′(0) and θ ′(0) in the PST scenario, as well as F ′(0), G ′(0) and θ(0) in the PHF scenario, respectively. The numerical result is derived from this calculation utilizing a step size of 0.001 and a convergence criterion of five decimal places.

5. Results and Analysis

A grey electrically conducting fluid flows hydromagnetically convective through a porous media with a spinning disk and an external uniform magnetic field. The numerical solutions address heat radiation, heat production and absorption, and these processes in relation to the fluid. Using the shooting approach in conjunction with a fourth-order Runge-Kutta integration methodology allows numerical solution of the system of equations. In accordance with the conditions at the border (15) level, which may fall anywhere from eleven to fourteen. Once numerical values have been ascribed to the parameters seen in the physical problem, a thorough comprehension of its radial velocity F, tangential velocity G, axial velocity H, and temperature θ has been achieved. To be more accurate, suction parameters should take on the values 1, -2, -3, and -4, while magnetic parameters should take on the values 1, 2, 3, and 4. The values of the following parameters are relevant to heat generation and absorption: -0.2, -0.1, 0.1, and 0.2: permeability, which indicates the degree to which a medium is permeable; radiation, which indicates the amount of heat radiated; and Prandtl number, which is 0.71 for air (where Pr = 0.71 denotes 20o C and one atmospheric pressure). Additionally, the Nusselt number, radial and tangential skin friction, and numerical method's accuracy were compared for the PST & (Pr = 0.71, M = 0.0, A= 0.0, L = 0.0, Rd = 109). This comparison was made in light of previously published data [29]. The comparative results, which are shown in Table 1, indicate a strong agreement. Table 2-13 highlights the behavior of the Nusselt numbers −θ'(0) (PST instance) and θ(0) (PHF instance) for specific values of the

International Research Journal on Advanced Engineering and Management
https://goldncloudpublications.com
https://doi.org/10.47392/IRJAEM.2025.0387
e ISSN: 2584-2854
Volume: 03
Issue:07 July 2025
Page No: 2456 - 2469

aforementioned governing factors, as well as the radial and tangential skin friction coefficients are defined as F ′ (0) and G ′ (0). (Figure 1,2,3,4,5,6)

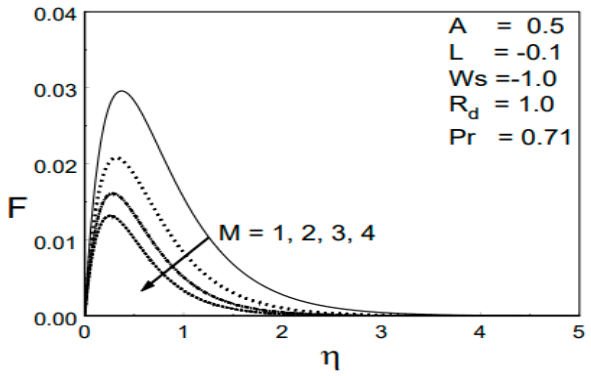

Fig.1 Impact of *M* on profiles of radial velocity

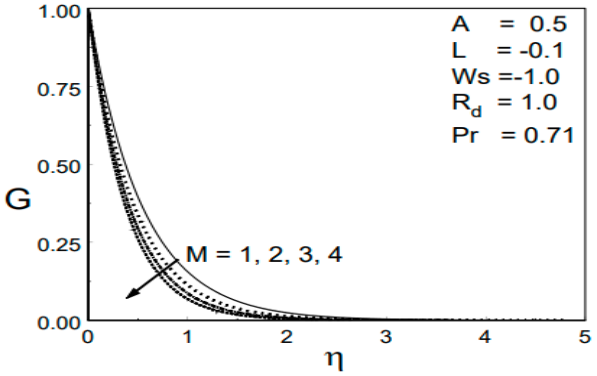

Fig.4 Impact of *M* on tangential velocity distributions

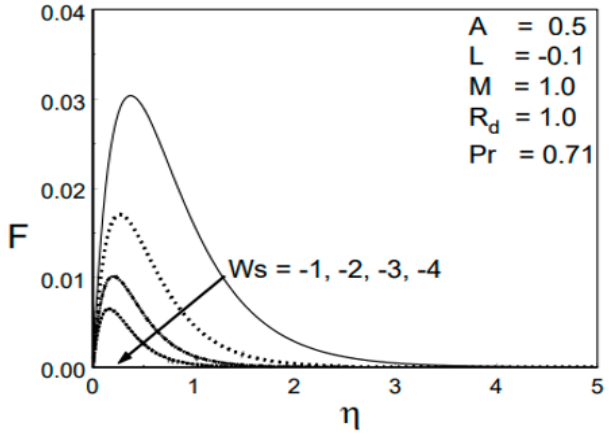

Fig.2 Impact of *Ws* on profiles of radial velocity

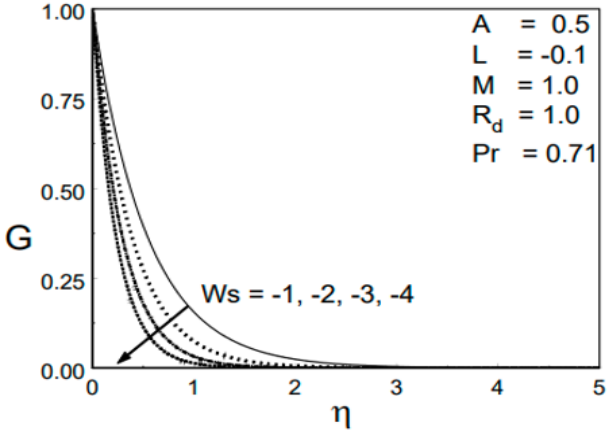

Fig.5 Impact of *Ws* on tangential velocity distributions

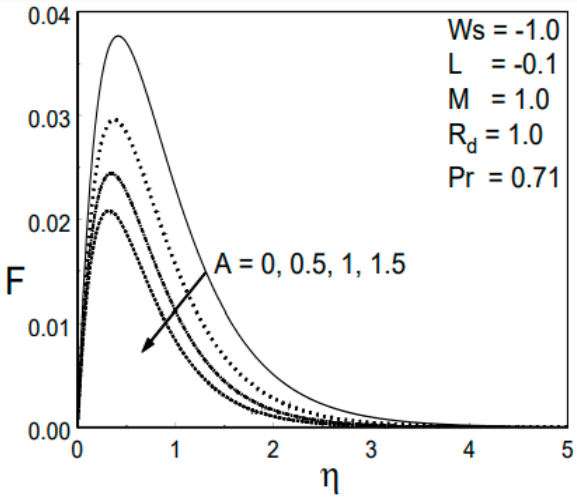

Fig.3 Impact of *A* on profiles of radial velocity

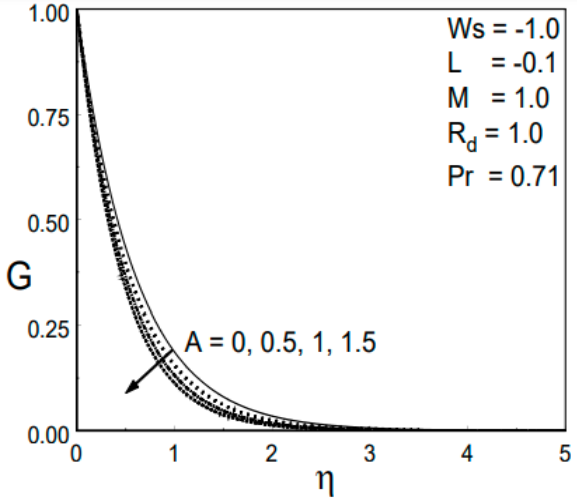

Fig.6 Impact of *A* on tangential velocity distributions

International Research Journal on Advanced Engineering and Management
https://goldncloudpublications.com
https://doi.org/10.47392/IRJAEM.2025.0387
e ISSN: 2584-2854
Volume: 03
Issue:07 July 2025
Page No: 2456 - 2469

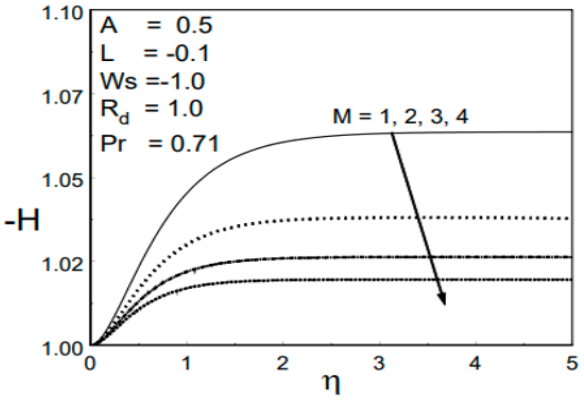

Fig.7 Impact of M on axial velocity distributions

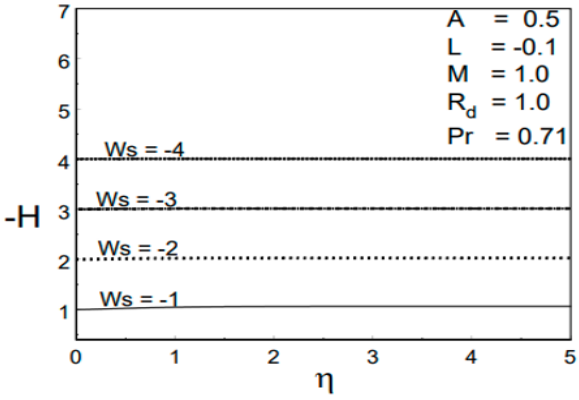

Fig.8 Impact of Ws on axial velocity distributions

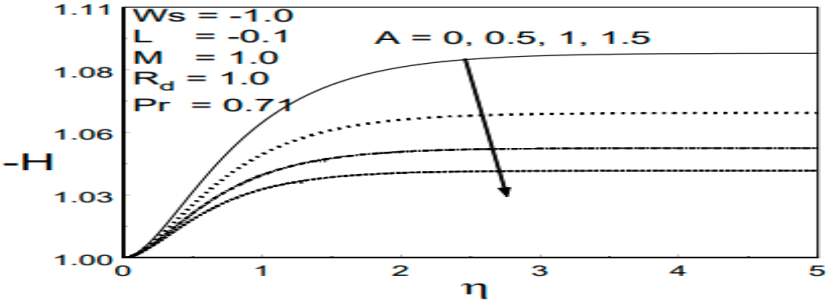

Fig.9 Impact of A on axial velocity distributions

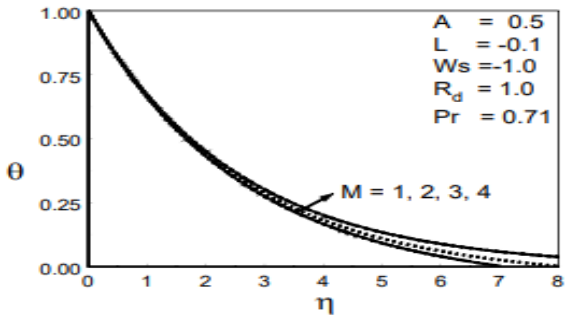

Fig.10 (PST Case)

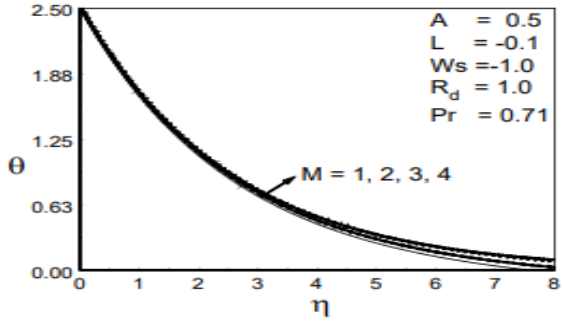

Fig.11 (PHF Case)

Impact of M on the distribution of temperatures

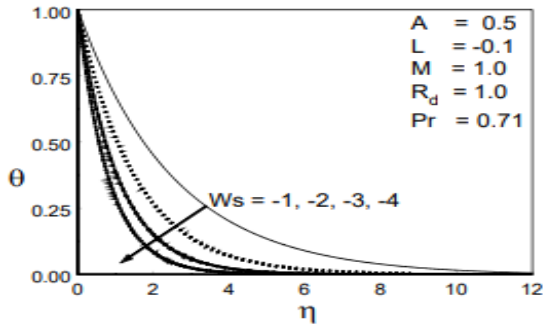

Fig.12 (PST Case)

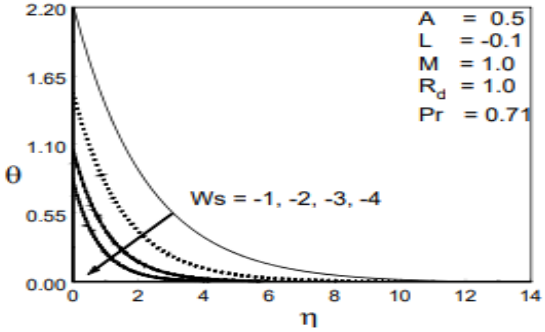

Fig.13 (PHF Case)

Impact of Ws on the distribution of temperature

International Research Journal on Advanced Engineering and Management
https://goldncloudpublications.com
https://doi.org/10.47392/IRJAEM.2025.0387
e ISSN: 2584-2854
Volume: 03
Issue:07 July 2025
Page No: 2456 - 2469

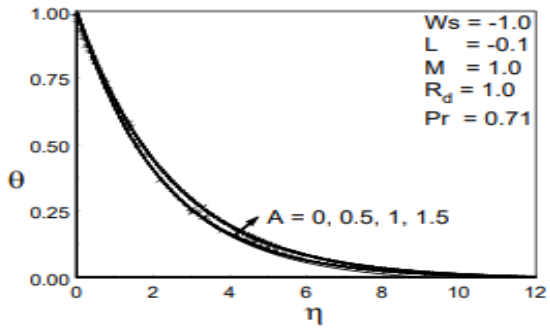

Fig.14 (PST Case)

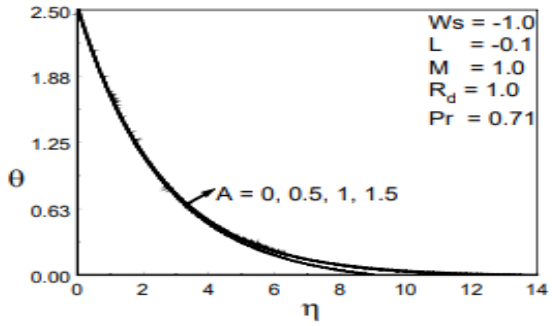

Fig.15 (PHF Case)

Impact of A on thermal distribution

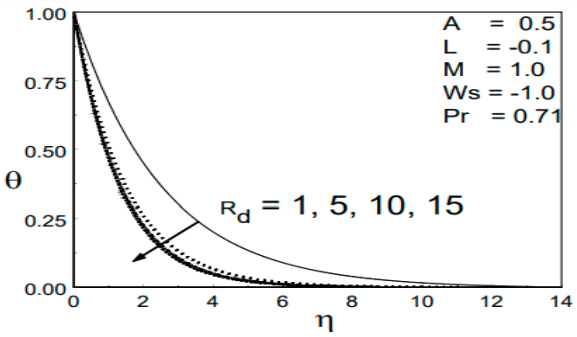

Fig.16 (PST Case)

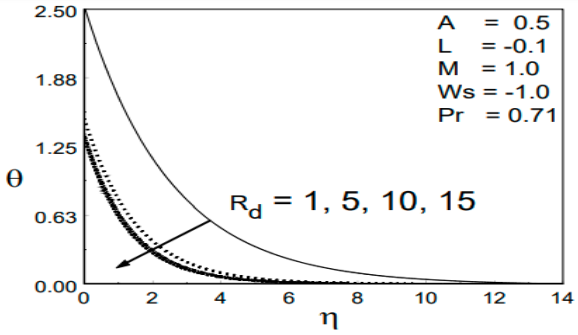

Fig.17 (PHF Case)

Impact of R_d on thermal distribution

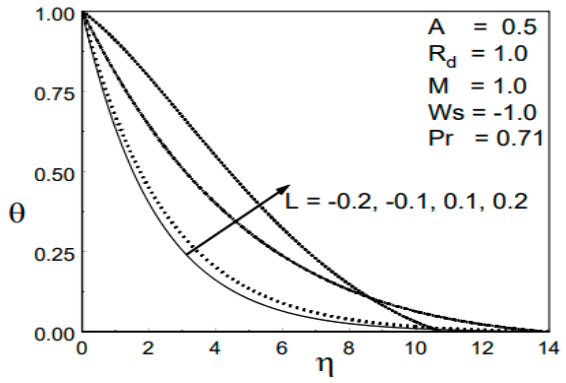

Fig.18 (PST Case)

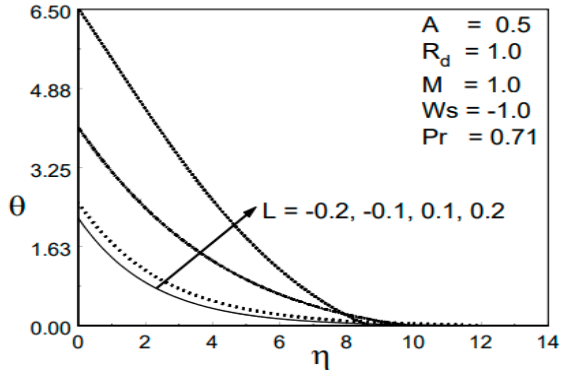

Fig.19 (PHF Case)

Impact of L on the distribution of temperatures

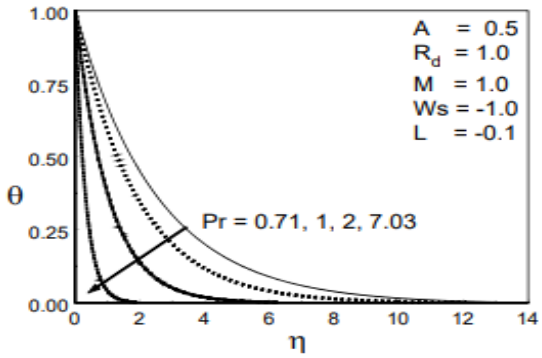

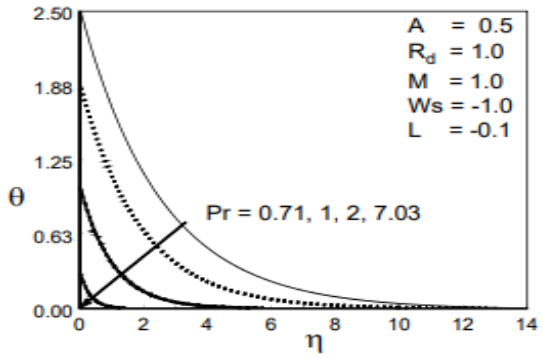

International Research Journal on Advanced Engineering and Management
https://goldncloudpublications.com
https://doi.org/10.47392/IRJAEM.2025.0387
e ISSN: 2584-2854
Volume: 03
Issue:07 July 2025
Page No: 2456 - 2469

W_s	Present			Kelson and Desseaux		
	$F'(0)$	$-G'(0)$	$-\theta'(0)$	$F'(0)$	$-G'(0)$	$-\theta'(0)$
4	0.243043	0.289210e-1	0.150101e-4	0.243044	0.289211e-1	0.107326e-4
3	0.309185	0.602989e-1	0.126771e-2	0.309147	0.602893e-1	0.576744e-3
2	0.398941	0.135959	0.116090e-1	0.398934	0.135952	0.110135e-1
1	0.489481	0.302173	0.850176e-1	0.489481	0.302173	0.848848e-1
0	0.510214	0.615926	0.326831	0.510233	0.615922	0.325856
-1	0.389564	1.175221	0.793069	0.389569	1.175222	0.793048
-2	0.242416	2.038527	1.437784	0.242421	2.038527	1.437782
-3	0.165576	3.012142	2.135586	0.165582	3.012142	2.135585
-4	0.124738	4.220518	2.842382	0.124742	4.005180	2.842381

Table 1. Comparison of, $F'(0), G'(0)$ & $-\theta'(0)$ for different values of W_s with $(Pr = 0.71, A = 0.0, M = 0.0, R_d = 10^9, L = 0.0)$

M	$F'(0)$	$-G'(0)$	$-\theta'(0)$
1	0.2195945	1.848522	0.3955877
2	0.1810917	2.172436	0.4014100
3	0.1577187	2.445736	0.4061409
4	0.1416300	2.686105	0.4070684

Table 2. (PST case)

M	$F'(0)$	$-G'(0)$	$\theta(0)$
1	0.2195945	1.848522	2.542044
2	0.1810917	2.172436	2.527882
3	0.1577187	2.445736	2.517240
4	0.1416300	2.686105	2.490987

Table 3. (PHF case)

Results of $F'(0), -G'(0)$ & $-\theta'(0)$ (For PST case) and $F'(0), -G'(0)$ & $\theta(0)$ (For PST case) for different values of M with $(A = 0.5, W_s = -1, R_d = 1, L = -0.1, Pr = 0.71)$.

W_s	$F'(0)$	$-G'(0)$	$-\theta'(0)$
-1	0.2195945	1.848522	0.3955877
-2	0.1728272	2.594124	0.6600636
-3	0.1364101	3.443018	0.9473602
-4	0.1105327	4.348722	1.242827

Table 4. (PST case)

W_s	$F'(0)$	$-G'(0)$	$\theta(0)$
-1	0.2195945	1.848522	2.542044
-2	0.1728273	2.594124	1.514691
-3	0.1364101	3.443017	1.055564
-4	0.1105327	4.348722	0.804617

Table 5. (PHF case)

Results of $F'(0), -G'(0)$ & $-\theta'(0)$ (For PST case) and $F'(0), -G'(0)$ & $\theta(0)$ (For PST case) for different values of W_s with $(A = 0.5, M = 1, R_d = 1, L = -0.1, Pr = 0.71)$.

International Research Journal on Advanced Engineering and Management
https://goldncloudpublications.com
https://doi.org/10.47392/IRJAEM.2025.0387
e ISSN: 2584-2854
Volume: 03
Issue:07 July 2025
Page No: 2456 - 2469

A	$F'(0)$	$-G'(0)$	$-\theta'(0)$
0	0.2510440	1.657076	0.4005608
0.5	0.2195945	1.848522	0.3975877
1	0.1975679	2.018473	0.3950058
1.5	0.1810914	2.172436	0.3943752

Table 6. (PST case)

A	$F'(0)$	$-G'(0)$	$\theta(0)$
0	0.2510440	1.657076	2.501996
0.5	0.2195943	1.848522	2.527882
1	0.1975679	2.018473	2.538024
1.5	0.1810914	2.172436	2.516337

Table 7. (PHF case)

Results of $F'(0)$, $-G'(0)$ & $-\theta'(0)$ (For PST case) and $F'(0)$, $-G'(0)$ & $\theta(0)$ (For PST case) for different values of A with ($W_s = -1, M = 1, R_d = 1, L = -0.1, Pr = 0.71$).

L	$F'(0)$	$-G'(0)$	$-\theta'(0)$
-0.2	0.2195945	1.848522	0.4518507
-0.1	0.2195945	1.848522	0.3955877
0.1	0.2195945	1.848522	0.2547453
0.2	0.2195945	1.848522	0.0964136

Table 10. (PST case)

L	$F'(0)$	$-G'(0)$	$\theta(0)$
-0.2	0.2195943	1.848522	2.211595
-0.1	0.2195943	1.848522	2.527882
0.1	0.2195943	1.848522	4.078546
0.2	0.2195943	1.848522	6.519483

Table 11. (PHF case)

Results of $F'(0)$, $-G'(0)$ & $-\theta'(0)$ (For PST case) and $F'(0)$, $-G'(0)$ & $\theta(0)$ (For PST case) for different values of L with ($W_s = -1, M = 1, A = 0.5, R_d = 1, Pr = 0.71$).

Pr	$F'(0)$	$-G'(0)$	$-\theta'(0)$
0.71	0.2195945	1.848522	0.3955877
1.0	0.2195945	1.848522	0.5275478
2.0	0.2195945	1.848522	0.9722018
7.03	0.2195945	1.848522	3.145561

Table 12. (PST case)

Pr	$F'(0)$	$-G'(0)$	$\theta(0)$
0.71	0.2195943	1.848522	2.527882
1.0	0.2195943	1.848522	1.895563
2.0	0.2195943	1.848522	1.028592
7.03	0.2195943	1.848522	0.317908

Table 13. (PHF case)

Results of $F'(0)$, $-G'(0)$ & $-\theta'(0)$ (For PST case) and $F'(0)$, $-G'(0)$ & $\theta(0)$ (For PST case) for different values of Pr with ($W_s = -1, M = 1, A = 0.5, L = -0.1, R_d = 1$).

As seen in Tables 2 and 3, Growing the magnetic field parameter M causes the rate of heat transfer −θ′(0) to increase in the PST scenario. Conversely, the surface temperature θ(0), tangential skin-friction G′(0), and radial skin-friction F′(0) all show a reduction in the PHF case. In relation to the suction parameter Ws, the surface temperature θ(0) (PHF), tangential skin-friction G′(0), and radial skin-friction F′(0) all rise. According to Tables 4 and 5, the rate of heat transfer −θ′(0) does not change in the PST scenario. A bigger velocity boundary layer is the result of a reduced surface velocity gradient, which is why blowing causes this. Results from Tables 6 and 7 demonstrate that as the porosity parameter A increases, there is a considerable decrease in the surface temperature θ(0), the rate of heat transfer −θ′(0), and the radial and tangential skin-friction coefficients F′(0) and G′(0). In the PST example, the Nusselt number −θ′(0) is shown in Table 8, while in the PHF case, the surface heat θ(0) is given in Table 9, for different values of Rd. Raising Rd causes a drop in surface temperature (PHF example) and Nusselt number (PST case). As the heat generation parameter L increases in the PHF instance, the surface heat θ(0) rises, whereas, the Nusselt number Nu falls in the PST. Tables 10 and 11 indicate this, which is a result of the heat-generating mechanism, which causes a layer of fluid to form close to the surface and causes its temperature to rise with time. For various values of Pr, Tables 12 and 13 display the differences between the surface heat θ(0) in PHF instance and Nusselt number −θ′(0) in the PST example. In the PHF scenario, surface

International Research Journal on Advanced Engineering and Management
https://goldncloudpublications.com
https://doi.org/10.47392/IRJAEM.2025.0387
e ISSN: 2584-2854
Volume: 03
Issue:07 July 2025
Page No: 2456 - 2469

temperature readings drop dramatically as the Prandtl number rises because the rate of heat transfer to the disc surface drops. An inverse relationship best describes the heat transfer rate. For different values of the magnetic parameter M, suction parameter Ws, and porous permeability parameter A, Figures 1-3 show the radial velocity profiles of the boundary layer F(η). As the strength of the applied z-direction magnetic field, which is perpendicular to the disc surface, increases, the radial velocity of the region decreases, as shown in Figure 1. This is because the hydromagnetic drag has increased. A maximum radial velocity is shown to occur at the disc's surface, followed by a rapid decrease to zero. Large suction results in a relatively modest radial velocity. The border layer is stabilized by suction, as Figure 2 makes evident. Figure 3 illustrates how the radial velocity distribution decreases as A increases. Fluid velocity falls when a porous substance is present because flow resistance rises. Figures 4-6 display tangential velocity profiles G(η) for different M, Ws, and A values. The thickness of the boundary layer of a porous material subjected to suction decreases as M increases. An example of a tangential magnetic force would be a flow with a tangential velocity G acting against a magnetic field B. Figure 4 shows that tangential velocities and boundary layer thickness both decrease as a result. The flow's azimuthal velocity decelerates even further when the Lorentz force is acting against it. In Figure 5, the impact of suction is seen by the tangential velocity profile. Rapid submersion of the surface occurs at high tangential velocities under intense suction. As A grows, the tangential velocity and boundary layer thickness both decreases, as demonstrated in Figure 6. Different values of M, Ws, and A are shown in Figures 7-9 for the steady state axial velocity profiles −H(η). If we increase the magnetic parameter M, as shown in Figure 7, the axial component of velocity will decrease. Now, consider the disk's surface with a suction applied, where Ws < 0. Aside from the pumping action of the fan on the rotating disc, additional pumping occurs due to the suction. There will be an increase in the quantity of fluid removed from the environment. The inflowing fluid now has two potential pathways to choose from. A radial rerouting of the inflow is also an option, in addition to continuing through the disk's suction holes. The easiest option will always be chosen. Getting free of the wall becomes increasingly easy as the suction increases. So, as Ws gets more negative, more and more of the input gets into the porous disc directly. This causes H to remain rather constant, as seen in Figure 8. The boundary layer expands as a result of an increase in axial velocity and an elevation in the porosity parameter, as illustrated in Fig. 9. Changes in temperature as a function of M, Ws, A, Rd, L, and Pr are shown in Figures 10 – 21. If we look at Figure 10 for the PST scenario and Figure 11 for the PHF scenario, we can see how the boundary layer temperature profiles are affected by the magnetic variable M. It is worth mentioning that M improves the local boundary layer temperature distribution, and the impact of the expanding magnetic variable is bigger close to the wall. Figure's 12 & 13 shows the border layer temperature profiles before and after adjusting the suction setting. Shortly after the application of wall suction (Ws < 0), Heat profiles and the thermal barrier layer both get thinner. The PST scenario (Figure 14) and the PHF scenario (Figure 15) show the impact of porosity parameter A on temperature θ. Which is produced by the fluid's near-ambient temperature not reaching the disc surface. This means that as M increases, the thermal boundary layer's thickness and temperature will also increase. Surfaces heated to around room temperature benefit from improved heat transmission in the absence of fluid. If the Figure 16 for the PST situation and Figure 17 for the PHF instance, where the radiation parameter Rd affects the temperature profile. Clearly, Rd affects the entire border layer. The remarkable thing is that Rd makes the thermal boundary layer's temperature distribution less. Since an increase in Rd decreases radiation, it indicates a lower temperature profile value in the thermal boundary layer. A fall in fluid temperature occurs when the thickness of the thermal boundary layer decreases as the radiation parameter increases., which in turn causes heat energy to be released from the flow zone. For the PST scenario, Figure 18 shows how the radiator/heat-sink parameter L influenced the temperature profiles of the boundary

International Research Journal on Advanced Engineering and Management
https://goldncloudpublications.com
https://doi.org/10.47392/IRJAEM.2025.0387
e ISSN: 2584-2854
Volume: 03
Issue:07 July 2025
Page No: 2456 - 2469

layer, and for the PHF instance, Figure 19 shows the same effect. It provides heat by forming a heated layer adjacent to the disk and reducing heating up the disk's exterior at a rate (L > 0). When cooling device (L < 0), also called heat absorption, is present, a cold layer of fluid forms next to the disc surface, which speeds up the removal of surface heat. Raising the quantity of thermal energy in the flow regime causes the temperature θ in the porosity regime to rise for L = 0.1, 0.2. Because L = -0.1, -0.2 results in lower temperatures, both the PST and PHF scenarios show heat absorption. In the boundary-layer domain, there is no temperature profile that deviates from zero as one approaches the edge. As illustrated in Figure 20 (PST instance) and Figure 21 (PHF case), different values of Pr cause changes in the temperature profiles when η is varied. Elevated Pr levels are able to lower body temperature. The actual behavior of the thermal boundary layer shrinks with increasing Pr, which is consistent with reality.

Conclusion

Thermodynamic boundary layer flow and heat transfer properties of an incompressible electrically conducting fluid across a porous rotating disk have been investigated using mathematical analysis within the framework of radiation and heat generation/absorption. Prescribed Surface Temperature (PST) and Prescribed Heat Flux (PHF) are two examples of possible scenarios involving heat transmission. An ordinary differential equation can be derived from a second-order momentum boundary layer problem that is significantly non-linear by employing von Karman similarity transformations. Integrating the firing methodology with the fourth-order Runge-Kutta method does not yield any numerical solutions to the momentum, continuity, and heat transfer equations. Heat generation / absorption characteristics, permeability, radiation, magnetism, and the Prandtl number are only a few of the numerous physical parameters examined to generate velocity and temperature profiles. From this investigation, the most crucial takeaways are:

- Raising the suction and magnetic field parameters in the PST case accelerates heat transfer, while in the PHF case lowering the surface temperature and tangential and radial skin friction leads to a cooler environment.
- Here, a small increase in the porosity parameter (PST) has a small but noticeable effect on the rate of heat conduction, radial and tangential skin friction, and surface temperature (PHF instance).
- Augmenting the porosity parameter (namely, PST) exerts a little yet discernible influence on the rates of heat conduction, radial and tangential skin friction, and surface temperature (PHF instance).
- Within the PST instance, Nusselt number goes up when the radiation parameter and Prandtl number go up. In the PHF case, it goes down as the surface temperature goes down.
- In the PST configuration, the Nusselt number increases as the heat source and sink parameters' values rise.
- As the magnetic field, suction, and porosity variables increase, the radial velocity decreases. Tangential velocity will decrease as the suction parameter, magnetic field, and porosity parameter rise.
- Parameters affecting magnetic interaction and porosity work in reverse of the way that the suction parameter accelerates the axial velocity.
- In cases where PST and PHF are involved, the temperature distribution is reduced by filtration, radiation, the Prandtl number, and heat sink characteristics (L < 0), and increased by magnetic interaction, porosity, and heat generation parameters (L > 0).

Both the heat transfer coefficient and the parameter for heat generation/absorption are improved in the PST scenario when the radiation parameter Rd and the Prandtl number Pr grow. Comparing the data trend for both scenarios with the same impacting characteristics, discovering that the PST case has a lower temperature at every point inside the border than the PHF scenario. Due to its increased cooling activity, PST is better than the other.

References

[1]. H.S. Takhar, A. Chamkha, G. Nath, Unsteady mixed convection flow from a rotating vertical cone with a magnetic field, Heat Mass

International Research Journal on Advanced Engineering and Management
https://goldncloudpublications.com
https://doi.org/10.47392/IRJAEM.2025.0387
e ISSN: 2584-2854
Volume: 03
Issue:07 July 2025
Page No: 2456 - 2469

Transfer 39 (2003) 297-304.
[2]. K.C.D.Hickman, Centrifugal boiler compression still, Indust. Engrg. Chem. 49 (1957) 786-800.
[3]. T.von Karman, Uber laminare und turbulente reibung, Z. Angew. Math. Mech. 1 (1921) 233-252.
[4]. J.T.Gregory, Stuart, W.S.Walker, On the stability of three dimensional boundary layers with applications to the flow due to a rotating-disk, Philos. Trans. R. Soc. London Ser. A 248 (1955) 155-199.
[5]. R.Benton Edward, On the flow due to a rotating disk, J. Fluid Mech. 24 (1966) 781-800.
[6]. P.Hall, An asymptotic investigation of the stationary modes of instability of the boundary layer on a rotating-disk, Proc. R. Soc. London Ser. A 406 (1986) 93-106.
[7]. O.A.Beg, H.S.Takhar, G.Nath, AJ.Chamkha., Mathematical modelling of hydromagnetic convection from a rotating sphere with impulsive motion and buoyancy effects, Nonlinear Analysis: Modelling and Control 11(3) (2006) 227-245.
[8]. Kh.Abdul Maleque, Md.Abdus Sattar, Steady laminar convective flow with variable properties due to a porous rotating disk, J. of Heat Transfer. 2005, Vol. 127.
[9]. M.Turkyilmazoglu, Exact solutions for the incompressible viscous fluid of a porous rotating disk flow, Int. J. of Non-Linear Mech. 44 (2009) 352-357.
[10]. T. Watanabe, I.Pop, Thermal boundary layers in magnetohydrodynamic flow over a flat plate in the presence of a transverse magnetic field, Acta Mech. 105 (1994) 233-238.
[11]. N.G.Kafoussias, N.D.Nanousis, Magnetohydrodynamic laminar boundary layer flow over a wedge with suction or injection, Can. J. Phys. 75 (1997) 733-745.
[12]. K.A.Yih, Forced convection flow adjacent to a non-isothermal wedge, Int. Commun. Heat Mass Transfer 26 (1996) 819-827.
[13]. H.A.Attia, A.Hassan, On hydromagnetic flow due to a rotating disk, Applied Mathematical Modelling 28 (2004) 1007-1014.
[14]. A.M. Rashad, Influence of radiation on MHD free convection from a vertical flat plate embedded in porous media with thermophoretic deposition of particles, Comm. Nonlinear Science Numerical Simulation 13 (10) (2008) 2213- 2222.
[15]. I.A.Hassanien , A.Y.Bakier, R.S.R.Gorla, Effect of thermal dispersion and stratification on non-darcy mixed convection from a vertical plate in a porous medium, Heat Mass Transfer 34 (1998) 2092-2112.
[16]. A.J.Chamkha , A.A.Khaled, Similarity solutions for hydromagnetic mixed convection heat and mass transfer for Hiemenz flow through porous media, Int. J. Numer. Meth. Heat Fluid Flow 10(1) (2000) 94-115.
[17]. H.A.Attia, Steady flow over a rotating disk in porous medium with heat transfer, Nonlinear Analysis: Modelling and Control 14(1) (2009) 21-26.
[18]. M.A.Hossain, H.S.Takhar, Radiation effect on mixed convection along a vertical plate with uniform surface temperature, Heat Mass Transfer 31(4) (1996) 243-248.
[19]. M.A.Hossain, I.Pop, Radiation effect on Darcy free convection in boundary layer flow along an inclined surface placed in porous media, Heat Mass Transfer 32(4) (1997) 223-227.
[20]. Z.Abbas, T.Hayat, Radiation effects on MHD flow in a porous space Int. J. of heat and mass transfer 51 (2008) 1024-1033.
[21]. H.S.Takhar, O.A.Beg, M.Kumari, Computational analysis of coupled radiation-convection dissipative non-gray gas flow in a non-Darcy porous medium using the Keller-Box implicit difference scheme, Int. J. Energy Research 22 (1998) 141-159.
[22]. A.J.Chamkha, Solar radiation assisted natural convection in a uniform porous medium supported by a vertical flat plate, ASME J. Heat Transfer 119 (1997) 89-96.
[23]. A.A.Mohammadein, M.A.Mansour, S.M.El Gaied, R.S.R.Gorla, Radative effect on

International Research Journal on Advanced Engineering and Management
https://goldncloudpublications.com
https://doi.org/10.47392/IRJAEM.2025.0387
e ISSN: 2584-2854
Volume: 03
Issue:07 July 2025
Page No: 2456 - 2469

natural convection flows in porous media, Transport Porous Media, 32(3) (1998) 263-283.

[24]. K.Vajravelu, J.Nayfeh, Hydromagnetic convection at a cone and a wedge, Int. Commun. Heat Mass Transfer 19 (1992) 701-710.

[25]. E.M.Abo-Eldahab, M.A.El Aziz, Blowing/suction effect on hydromagnetic heat transfer by mixed convection from an inclined continuously stretching surface with internal heat generation/absorption, Int. J. Therm. Sci. 43 (2004) 709-719.

[26]. A.J.Chamkha, Thermal radiation and buoyancy effects on hydromagnetic flow over an accelerating permeable surface with heat source or sink, Int. J. of Engineering Sci. 38 (2000) 1699-1712.

[27]. M.Molla, M.Hossain, M.Taher, Magnetohydrodynamic natural convection flow on a sphere with uniform heat flux in presence of heat generation, Acta Mechanica 186 (2006) 75-86.

[28]. B.Sahoo, Effects of slip, viscous dissipation and joule heating on the MHD flow and heat transfer of a second grade fluid past s radially stretching sheet, Applied Mathematics and Mechanics 31(2) (2010) 159-173.

[29]. N.Kelson and A.Desseaux, Note on porous rotating disk flow, ANZIAM J., 42 (2000) C847-C855.

[30]. R. Ellahi, M.H. Tariq, M. Hassan, K. Vafai, On boundary layer nano-ferroliquid flow under the influence of low oscillating stretchable rotating disk, Journal of Molecular Liquids 229 (2017) 339-345.

[31]. Mahabaleshwar, U S et al. The MHD Newtonian hybrid nanofluid flow and mass transfer analysis due to superlinear stretching sheet embedded in porous medium, Scientific reports 11, (2021) 1 22518.

[32]. Mubashar Arshad, MHD hybrid nanofluid flow in a rotating system with an inclined magnetic field and thermal radiation, Case Studies in Thermal Engineering 62 (2024) 105182.

[33]. Eswari, L. Maragatham, N. Anbazhagan, Gyanendra Prasad Joshi, Woong Cho, Analytical investigation of heat and mass transfer in MHD nano fluid flow past a moving vertical plate, Case Studies in Thermal Engineering 60 (2024) 104642.